APPLIED AND ENVIRONMENTAL MICROBIOLOGY, Oct. 2007, p. 6125–6133 Vol. 73, No. 19
0099-2240/07/$08.00+0 doi:10.1128/AEM.00608-07

agr System of *Listeria monocytogenes* EGD-e: Role in Adherence and Differential Expression Pattern[▽]

Aurélie Rieu,[1] Stéphanie Weidmann,[2] Dominique Garmyn,[1] Pascal Piveteau,[1]* and Jean Guzzo[2]

UMR 1229 Microbiologie du Sol et de l'Environnement, Université de Bourgogne, INRA, F-21000 Dijon, France,[1] and Laboratoire REVV, Université de Bourgogne, IUVV, F-21000 Dijon, France[2]

Received 16 March 2007/Accepted 27 July 2007

In this study, we investigated the *agrBDCA* operon in the pathogenic bacterium *Listeria monocytogenes* EGD-e. In-frame deletion of *agrA* and *agrD* resulted in an altered adherence and biofilm formation on abiotic surfaces, suggesting the involvement of the *agr* system of *L. monocytogenes* during the early stages of biofilm formation. Real-time PCR experiments indicated that the transcript levels of *agrBDCA* depended on the stage of biofilm development, since the levels were lower after the initial attachment period than during biofilm growth, whereas transcription during planktonic growth was not growth phase dependent. The mRNA quantification data also suggested that the *agr* system was autoregulated and pointed to a differential expression of the *agr* genes during sessile and planktonic growth. Although the reverse transcription-PCR experiments revealed that the four genes were transcribed as a single messenger, chemical half-life and 5′ RACE (rapid amplification of cDNA ends) experiments indicated that the full size transcript underwent cleavage followed by degradation of the *agrC* and *agrA* transcripts, which suggests a complex regulation of *agr* transcription.

Listeria monocytogenes is a gram-positive human pathogenic bacterium; it is the causative agent of listeriosis, a serious infection characterized by high mortality rates, in immunocompromised individuals and pregnant women (19). This pathogenic bacterium is widely spread in the environment (soil, vegetation, animals, farm environment, etc.). In connection with these extended reservoirs, *L. monocytogenes* is also a contaminant of the food industry. Its presence on working surfaces in food-processing plants is a major problem as a source of food contamination (1, 32). Like most bacteria, *L. monocytogenes* is able to colonize surfaces and form biofilms (sessile growth) while, in natural environments, free-floating cells (planktonic growth) are transitory (28). Several steps can be identified during biofilm development: after an initial step of reversible and then irreversible adherence, bacteria grow as microcolonies and spread on the surface. Finally, biofilms develop as complex, three-dimensional structures during the maturation step (17). Biofilm development and maturation requires complex cellular mechanisms in which cell-cell communication is involved (14, 30). To date, three major signaling systems have been identified; to regulate these systems, bacterial extracellular signaling molecules called autoinducers are produced (8). The acylhomoserine lactones have been identified as autoinducers in gram-negative bacteria (3, 13, 27, 46). The autoinducer 2 is found in both gram-negative and gram-positive bacteria (5, 7, 11, 35, 36, 54). Finally, peptide-mediated signaling pathways have been characterized in gram-positive bacteria. Among these, the *agr* system has been described initially in *Staphylococcus aureus* (41); the production of many of its virulence factors (toxins, enzymes, and cell surface proteins) is regulated by this system (4). The role of the *agr* system during *S. aureus* biofilm development is complex (57). It depends on the hydrodynamic conditions of the experimental setup. Under static conditions *agr* expression reduces the attachment of the cells to the surface (52, 55), and under turbulent dynamic conditions *agr* expression may affect biofilm maturation (55). Orthologs of the *agr* system have also been described in *Enterococcus faecalis* (*fsr*) (45), *Lactobacillus plantarum* (*lam*) (48), and *L. monocytogenes* (*agr*) (6). In *E. faecalis*, expression of a gelatinase (GelE) is *fsr* dependent (45). In *L. plantarum*, the *lam* system plays a role during biofilm development (48).

In *L. monocytogenes*, the four genes (*agrB*, *agrD*, *agrC*, and *agrA*) of the *agr* locus are organized as an operon (Fig. 1A). They encode the two-component histidine kinase AgrC and response regulator AgrA, a precursor peptide AgrD and AgrB, a protein that is involved in the processing of AgrD into a matured autoinducing peptide. Limited data concerning the role of the *agr* locus on the physiology of *L. monocytogenes* are available. Williams et al. (53) showed that among 16 putative response regulator genes of *L. monocytogenes* EGD-e, in-frame deletion in *agrA* did not affect the growth in brain heart infusion (BHI) medium at various temperatures (20, 37, and 43°C), in the presence of 9% NaCl, 5% ethanol, or 0.025% H_2O_2. Swimming motility was also not affected. No alteration of virulence could be identified during in vitro infection of cell cultures nor in vivo after intravenous infection of BALB/c mice. In a previous study, Autret et al. (6) reported a moderate attenuation of the virulence in Swiss mice after insertion of Tn*1545* in the *L. monocytogenes* EGD-e *agrA* gene.

To further elucidate the role of the *agr* system, we first of all examined its involvement during attachment to abiotic surfaces and biofilm growth. *agrA* and *agrD* in-frame deletion mutants were compared to the parental strain EGD-e during sessile growth. Second, we determined the expression pattern of the four genes of the *agr* operon during planktonic and sessile growth, and we evidenced posttranscriptional events during expression of this operon.

* Corresponding author. Mailing address: UMR 1229 Microbiologie du Sol et de l'Environnement, Université de Bourgogne, INRA, F-21000 Dijon, France. Phone: 33 3 80 39 68 93. Fax: 33 3 80 39 39 55. E-mail: piveteau@u-bourgogne.fr.

▽ Published ahead of print on 3 August 2007.

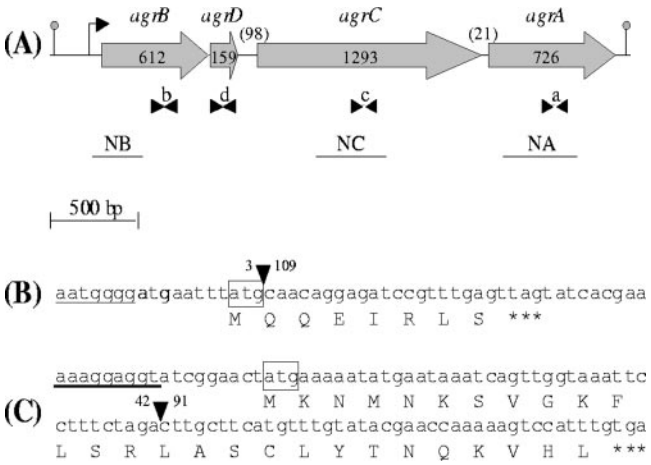

FIG. 1. (A) Schematic diagram of *L. monocytogenes agr* operon. The gray arrows indicate the orientation and the size in base pairs of the four genes. Numbers between parentheses indicate the size in base pairs of the two intergenic regions. Arrowheads indicate the positions of the oligonucleotides used for real-time PCR: b (BR2; BF2), d (DF2; DR2), c (CF2; CR2), and a (AF2; AR2). The black lines indicate the probes used for Northern blotting (NB, NC, and NA). The position of the transcription initiation site and the transcription termination site are indicated, respectively, by the bent arrow and the gray dot. (B and C) DNA and deduced amino acid sequences of *agrA* gene containing a 106-bp deletion in DG125A (Δ*agrA*) mutant (B) and of *agrD* gene containing a 49-bp deletion in DG119D (Δ*agrD*) mutant (C). The position of the deletion is represented by an inverted black triangle, the nucleotides before and after the deletion are mentioned, the ribosome binding sites are underlined, the start codons are boxed, and the stop codon is represented by three asterisks.

MATERIALS AND METHODS

Bacterial strains and growth media. The bacterial strains and plasmids used in the present study and their characteristics are shown in Table 1. *L. monocytogenes* EGD-e, isolated from a rabbit listeriosis outbreak (39), and two mutants, derivatives of *L. monocytogenes* EGD-e, *L. monocytogenes* DG119D (Δ*agrD*) and *L. monocytogenes* DG125A (Δ*agrA*) were grown in tryptic soy broth (TSB; Biokar Diagnostics, Pantin, France) at 25°C for biofilm and planktonic cultures and in brain heart infusion broth (BHI; Biokar Diagnostics) at 40°C for mutant construction. *Escherichia coli* TOP10 and Match1 (Invitrogen, Cergy Pontoise, France) were grown aerobically in Luria-Bertani broth (LB; Biokar Diagnostics) at 37°C. When appropriate, antibiotics (Sigma, St. Quentin Fallavier, France) were added as follows: kanamycin, 50 μg ml^{-1} (*E. coli*); ampicillin, 200 μg ml^{-1} (*E. coli*); and chloramphenicol, 10 μg ml^{-1} (*L. monocytogenes*) (Table 1).

In-frame deletion of *agrD* and *agrA* genes. The mutant strains listed in Table 1, carrying an in-frame deletion in the response regulator *agrA* or in the precursor peptide *agrD* genes, were constructed from the parental strain *L. monocytogenes* EGD-e by using a two-step integration/excision procedure (10) that is based on the mutagenesis plasmid pGF-EM (33).

First, for the construction of an *agrA* in-frame deletion mutant, primers C13 and A12 (Table 2) were used to amplify a 600-bp DNA fragment including the 3′ end of *agrC* and the ATG of *agrA*. The PCR product was cloned into pGF-EM (33) after digesting this PCR product and vector with HindIII/XbaI. The resulting plasmid, pGID121 was transformed into chemically competent *E. coli* Match1 as recommended by the manufacturer (Invitrogen). Primers A15 and E2 (Table 2) were used to amplify a 500-bp internal fragment of *agrA*. The resulting fragment was cloned into pCR2.1 TOPO vector (Invitrogen) to obtain plasmid pGID118. This vector was transferred into *E. coli* TOP10. Plasmid pGID118 was digested with NheI/EcoRI and the resulting 500-bp fragment containing an internal part of *agrA* was ligated into pGID121 restricted with XbaI/EcoRI to obtain pGID125. This plasmid was electroporated into *L. monocytogenes* EGD-e.

Second, a similar strategy was used for the construction of an *agrD* in-frame deletion mutant. Primers D1 and D2 (Table 2) were used to amplify a 400-bp DNA fragment including the 5′ end of *agrD*. The PCR product was cloned into pGF-EM (33) to obtain pGID112. Primers D3 and D4 (Table 2) were used to amplify a 600-bp DNA fragment including the 3′ end of *agrD* and the 5′ end of *agrC*. The resulting fragment was cloned into pCR2.1 TOPO vector (Invitrogen) to obtain plasmid pGID109. After digestion, the plasmid pGID109 was ligated into digested plasmid pGID112 to obtain pGID119. This plasmid was electroporated into *L. monocytogenes* EGD-e.

Finally, transformants were selected on BHI agar plates (Biokar Diagnostics) containing 10 μg of chloramphenicol (Sigma) ml^{-1}. A transformant was serially subcultured in BHI at 40°C to direct chromosomal integration of the plasmid by homologous recombination. Chromosomal integration was confirmed by PCR and a single colony, with a chromosomal integration, was serially subcultured in BHI at 40°C and screened for loss of chloramphenicol resistance. Allelic exchange mutagenesis was confirmed by PCR amplification and direct sequencing of the PCR product (GENOME Express, Meylan, France). The mutants selected were named DG125A (Δ*agrA*) and DG119D (Δ*agrD*). The deletion of 106 bp in

TABLE 1. Bacterial strains and plasmids used in this study

Bacterial strain or plasmid	Relevant property[a]	Source or reference
Strains		
E. coli TOP10	Cloning host	Invitrogen
E. coli Match1	Cloning host	Invitrogen
L. monocytogenes EGD-e	Wild type of serotype 1/2a for which the genome sequence is available	39
L. monocytogenes DG125A	*L. monocytogenes* EGD-e with in-frame deletion of the *agrA* gene	This work
L. monocytogenes DG119D	*L. monocytogenes* EGD-e with in-frame deletion of the *agrD* gene	This work
Plasmids		
pGF-EM	Cm^r Am^r; 9.4-kb derivative of pCON-1 containing the 0.8-kb *gfp* gene of pKV111 and the *erm* gene of Tn*917*	33
pGID109	Km^r Am^r; 4.4-kb derivative of pCR21-TOPO containing the 0.6-kp 3′ end of *agrD* and the 5′ end of *agrC*	This work
pGID112	Cm^r Am^r; 10.4-kb derivative of pGF-EM containing the 0.4-kb 5′ end of *agrD*	This work
pGID118	Km^r Am^r; 4.3-kb derivative of pCR21-TOPO containing the 0.5-kp internal region of *agrA*	This work
pGID119	Cm^r Am^r; 9,4-kb derivative of pGID112 containing the 3′ end of *agrD* inserted into the XbaI/EcoRI site of pGID109	This work
pGID121	Cm^r Am^r; 10.6-kb derivative of pGF-EM containing the 0.6-kb 3′ end of *agrC* and the ATG of *agrA*	This work
pGID125	Cm^r Am^r; 9.3-kb derivative of pGID121 containing the internal region of *agrA* inserted into the XbaI/EcoRI site of pGID118	This work

[a] Km^r, kanamycin resistant; Am^r, ampicillin resistant; Cm^r, chloramphenicol resistant.

TABLE 2. Oligonucleotides used in this study

Description and application[a]	Sequence (5′→3′)[b]	Created restriction site	Primer
Constructions			
pGID121	**AAAGCTT**CGCGTTTTTCGTCATGATT	HindIII	C13
	ATCTAGACATAAATTCATCCCCATTCT	XbaI	A12
pGID118	**AGCTAGC**AACAGGAGATCCGTTTGAG	NheI	A15
	CTTACCATAAAATTCCACTT		E2
pGID112	CA**AAGCTT**TTACTGCAAACA	HindIII	D1
	AAGAATCCGCAACTTTCATGG		D2
pGID109	CTATGAG**TCTAGA**TTGCTTCATG	XbaI	D3
	AACAAATTCGCCAACATTCC		D4
RNA analysis			
qRT-PCR *drm*	GCGGAAAAACCACTTGCTTACT		DRMF2
	CGGAAAGGTGTGTCAATGTATAGG		DRMR2
qRT-PCR *agrB*	CGGCAGACACAGAAAGTTTG		BF2
	TGCGAATGGTATTAGCAACG		BR2
qRT-PCR *agrD*	AAATCAGTTGGTAAATTCCTTTCTAG		DF2
	AATGGACTTTTTGGTTCGTATACA		DR2
qRT-PCR *agrC*	GGGGTCAATCGCAGGTTTTG		CF2
	CTTTAAGTTCGTTGGTTGCCGTA		CR2
qRT-PCR *agrA*	GCAAGCAGAAGAACGATTTCCAA		AF2
	CGCTGTCTCAAAAAACAAGATAT		AR2
RT-PCR *agrBD*	CA**AAGCTT**TTACTGCAAACA	HindIII	D1
	TTGCATTTTCACAAATGGACTT		DR
RT-PCR *agrDC*	CCATGAAAGTTGCGGATTCT		DF
	GGCACTTACAAAAACAATCAATAC		C35
RT-PCR *agrC* and Northern blot *agrC*	GGAATGTTGGCGAATTTGTT		C11
	CTTCAAACCCGGCATATCAT		C10
RT-PCR *agrCA*	CAAAAGGAGAAGGTCGTGGA		C23
	ACCATTCATGTCCGGCTGCC		A46
Northern blot *agrB*	A**CCATGG**GTAAATTCGTTGTAAAATA	NcoI	B17
	CGTGCAATTCAATGTTTTGG		BR
Northern blot *agrA*	A**GCTAGC**AACAGGAGATCCGTTTGAG	NheI	A15
	CTTACCATAAAATTCCACTT		E2
5′RACE *agrB*	TGCGAATGGTATTAGCAACG		BR2
	CGAAATCAACACATCCGCCAT		B34
5′RACE *agrC*	GGCACTTACAAAAACAATCAATAC		C35
	CTAAAGTAAATAAAGGGAAGGCTA		C36
5′RACE *agrA*	TTGATGTGTAGGCATTCGTG		A44
	ACCATTCATGTCCGGCTGCC		A46
	CGCTGCATTCTGTTATCTTCA		A48
	CTTCAATATATTTCGTTAACCT		A50
Primer extension *agrB*	GACAAAGGGACTTTTGCAGT		B18
	CTTCTTCATCATCTTTCCAGCG		B26
	CGAAATCAACACATCCGCCAT		B34

[a] qRT-PCR, quantitative RT-PCR.
[b] Specific restriction sites are underlined, and extra nucleotides added to include restriction sites to the PCR product are indicated in boldface.

strain DG125A (Δ*agrA*) (Fig. 1B) and the deletion of 49 bp in strain DG119D (Δ*agrD*) (Fig. 1C) resulted in a frameshift causing the premature appearance of a stop codon and thus the premature stop of translation.

Adhesion on glass slide. An overnight culture of the bacterium in TSB was used to inoculate (1/100, vol/vol) fresh TSB and was grown at 25°C to an optical density at 600 nm of 0.1. A portion (5 μl) of the culture to be tested was then deposited on a glass slide, and the glass slide was incubated for 2 h at 25°C. After incubation, the glass slide was washed twice in distilled water and the adhering cells were stained with a 0.1% (wt/vol) aqueous crystal violet solution for 1 min and washed with distilled water. Adhering cells were observed by using a Zeiss Axioplan 2 imaging microscope. For each experiment, 12 replicates resulting from three independent inocula were analyzed.

Biofilm formation on polystyrene microplate. An overnight culture of the bacterium in TSB at 25°C was used to inoculate (1/100, vol/vol) fresh TSB. A total of 100 μl per well was dispensed on a 96-well microtiter plate (Nunc, Dominique Dutscher S.A., Brumath, France), which was then incubated at 25°C for 16 to 72 h. Cells attached to the well walls were quantified as previously described (16) with some modifications. After incubation, the medium was removed from each well, and the plates were washed twice by using a microtiter plate washer (Cellwash; Thermolabsystems, Cergy Pontoise, France) with 100 μl of 150 mM NaCl solution in order to remove loosely attached cells. The plates were then stained with a 0.05% (wt/vol) aqueous crystal violet solution for 45 min and washed three times. In order to quantitatively assess biofilm production, 100 μl of 96% ethanol (vol/vol) were added to each well, and the optical density at 595 nm (OD_{595}) was determined. For each experiment, 15 replicates resulting from three independent inocula were analyzed. Each microtiter plate included eight wells with sterile TSB as control.

Biofilm formation on stainless steel chips. AISI 304 stainless steel chips of 8-cm diameter (Goodfellow SARL, Lille, France) were inserted in petri dishes containing 20 ml of inoculated TSB (1/100, vol/vol), followed by incubation at 25°C for 2 h to allow adhesion. For biofilm development, the medium was removed, and 20 ml of fresh TSB was added. Biofilms were grown for 24 and 72 h at 25°C. After incubation, the medium was removed, and 10 ml of saline solution (150 mM NaCl) was softly poured twice onto chips, followed by agitation for 1 min on an orbital shaker at 240 rpm (IKAKS 130 basic) to remove loosely adhering bacteria. Sessile cells were detached from chips in 10 ml of saline solution by scraping with a sterile disposable cell lifter (TPP; Dominique Dutscher S.A.).

RNA extraction and cDNA preparation. Cells were harvested by centrifugation (10,000 × *g*, 5 min), resuspended in 1 ml of Tri-reagent (Sigma), and disrupted with glass beads (106 μm) in a FastPrep FP120 instrument (Thermo Savant-Bio

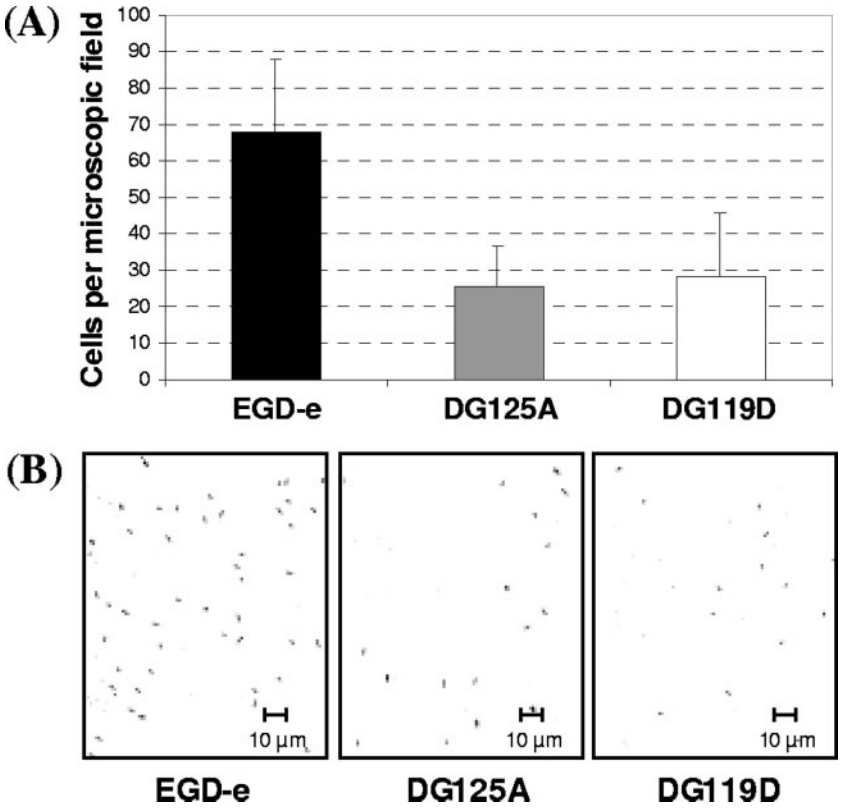

FIG. 2. (A) *L. monocytogenes* EGD-e (■), DG125A (Δ*agrA*) (▨), and DG119D (Δ*agrD*) (□) cell adhesion after 2 h of incubation at 25°C on glass slides. Histograms represent the number of adhered cells counted per microscopic field. Each bar indicates the mean of three independent experiments with four microscopic fields per experiment. (B) Micrographs of microscopic fields showing *L. monocytogenes* EGD-e, DG125A (Δ*agrA*), and DG119D (Δ*agrD*) cells adhering to glass slides after 2 h of incubation at 25°C. Magnification, ×63.

101) at 4°C for eight rounds of 30 s at 6,000 × *g*. Nucleic acids were extracted twice in 0.2 volume of chloroform and purified by precipitation in 1 volume of isopropanol. RNA pellets were dried and resuspended in 80 μl of RNase-free water. Nucleic acid concentrations were calculated by measuring the absorbance at 260 nm using a SmartSpec Plus spectrophotometer (Bio-Rad, Marnes La Coquette, France).

Before reverse transcription (RT), 2 μg of total RNA were treated with 2 U of DNase (Invitrogen) as described by the manufacturer. The absence of chromosomal DNA contamination was checked by real-time PCR. cDNA were then synthesized by using an iScript cDNA synthesis kit (Bio-Rad) as recommended.

Real-time PCR experiments. Real-time PCR as described by Desroche et al. (15) was used to quantify mRNA levels. Gene-specific primers (Table 2 and Fig. 1A) were designed to amplify cDNAs of the transcripts of *agrB*, *agrD*, *agrC*, and *agrA* with the Bio-Rad SYBR green kit in a Bio-Rad I-Cycler. These gene-specific primers were designed outside zones of deletion, allowing the determination of the transcript levels of the *agrB*, *agrD*, *agrC*, and *agrA* genes in the parental strain and in both mutants DG125A (Δ*agrA*) and DG119D (Δ*agrD*). This method was used to analyze their mRNA level during planktonic growth at early exponential phase (6.5×10^7 CFU ml^{-1}; OD_{600} of 0.1), mid-exponential phase (2.5×10^8 CFU ml^{-1}; OD_{600} of 0.4), and stationary phase (4×10^8 CFU ml^{-1}; OD_{600} of 0.6) and after 2, 24, and 72 h of biofilm formation on AISI 304 stainless steel chips. The specificity of each primer pair was controlled by melting curves, and the mean of efficiencies for the five primer pairs was 98% ± 9%. The results were analyzed by using the comparative critical threshold method ($\Delta\Delta C_T$) in which the amount of targeted mRNA was first of all normalized using a specific mRNA standard and then compared to a calibrator condition (15). *drm*, a gene coding for a phosphopentomutase, was selected as an internal standard since *drm* transcript levels were stable in the conditions tested. For our work, the calibrator condition corresponded to the *agrA* mRNA level at an OD_{600} of 0.1. The relative level of *agrA* mRNA at an OD_{600} of 0.1 thus corresponded to 1. mRNA quantification was performed in triplicate from total RNA extracted from three independent cultures.

RT-PCR. RT-PCR were performed with cDNA synthesized with total RNA extracted from three different mid-exponential phase cultures (OD_{600} of 0.4) as described above. Specific primers (Table 2) were designed to amplify transcripts of the four genes and the two intergenic regions. PCR products were separated by electrophoresis on a 1% agarose gel (Invitrogen). Samples were checked for DNA contamination by performing PCR prior to RT.

Northern blotting. Northern blot analysis were performed by fractionation of RNA samples on 1% (wt/vol) agarose gel containing 20% (wt/vol) formaldehyde. Then, 30 μg of total RNA was loaded into each well of the gel. Transfer to a nylon membrane (Hybond-N; Amersham, Orsay, France) was performed as recommended. Internal probes (Fig. 1A) of the *agrB*, *agrC*, and *agrA* genes were generated by PCR using primers described in Table 2. Portions (10 ng) of the PCR products were labeled with [α-^{32}P]dATP (Amersham) by the random priming method according to the manufacturer's instructions (Invitrogen) to produce specific RNA probes. Sizes were determined with a RNA ladder (Invitrogen) as the molecular weight standard.

mRNA chemical half-life determination. The chemical half-lives of mRNA of the four genes of the *agr* operon were determined from mid-exponential phase cultures (OD_{600} of 0.4). Total RNA was isolated as described above from samples taken 1, 4, 7, and 10 min after rifampin treatment (250 μg ml^{-1}; Sigma). The half-life was determined for each gene by real-time PCR using the time at which rifampin was added as a calibrator and the 16S rRNA transcript levels as an internal standard.

Analysis of the 5′ end of *agr* mRNA. Primer extensions were performed by incubating 5 μg of RNA isolated from *L. monocytogenes* cells in planktonic growth, 20 pmol of oligonucleotide, 92 GBq of [α-^{32}P]dATP (Perkin-Elmer, Courtaboeuf, France), and 100 U of SuperScript II reverse transcriptase (Invitrogen). The oligonucleotides used in this experiment are described in Table 2. The corresponding DNA-sequencing reactions were carried out using the primers and Cycle Reader DNA sequencing kit as recommended by the manufacturer (Fermentas, Euromedex, Souffel Weyersheim, France).

A capping assay was used to distinguish 5′ triphosphate (indicating initiation

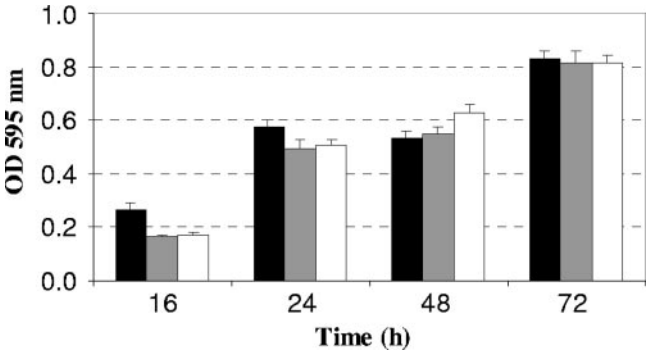

FIG. 3. Biofilm formation by *L. monocytogenes* EGD-e (■), DG125A (Δ*agrA*) (▨), and DG119D (Δ*agrD*) (□) in batch conditions in polystyrene 96-well plates after 16, 24, 48, and 72 h of incubation at 25°C. Each histogram indicates the mean of three independent experiments, with five measurements for each point.

points) from 5′ monophosphate (indicating processed products) according to the method of Bensing et al. (9), using a 5′-RACE kit (Ambion; Applied Biosystems, Courtaboeuf, France). Only 5′ monophosphate are selectively ligated to an RNA oligonucleotide. The primary 5′ end may be ligated only after removal of a 5′ pyrophosphate through tobacco acid pyrophosphatase (TAP) activity. The oligonucleotides used in this experiment are described in Table 2. Sequencing of 5′-RACE products obtained from TAP-treated and nontreated RNA was performed to differentiate cleavage products from primary transcripts. Primers used for PCR amplification between adaptor and the gene of interest are described in Table 2. PCR products were sequenced by GENOME express.

Statistical analysis. A one-way analysis of variance was performed by using SigmaStat version 3.0.1 software (SPSS, Inc.) in order to test the significance of the differences (i) in gene expression during planktonic growth and biofilm formation using the ΔC_T value and (ii) in biofilm quantity. When one-way analysis of variance was significant, the Holm-Sidak test ($n = 3$, $P < 0.05$) was used to locate significant differences.

Nucleotide sequence accession numbers. The DNA sequence data of the mutant strains described in the present study have been deposited in GenBank/EMBL/DDBJ under the accession numbers AM412557 and AM412558.

RESULTS

The *agr* operon is involved during the sessile growth of *L. monocytogenes* EGD-e. In order to study the involvement of the putative transcriptional regulator AgrA during sessile growth, an *agrA* in-frame deletion mutant of *L. monocytogenes* EGD-e was constructed. As expected, this mutation did not alter cell or colony morphology or planktonic growth (data not shown). In contrast, the glass slide adherence of mutant DG125A (Δ*agrA*) was affected. Indeed, the number of adhered cells of DG125A was significantly reduced ($n = 3$, $P < 0.05$) by 62% compared to the parental strain EGD-e (Fig. 2A). Since cell-cell communication affects biofilm formation in many bacterial species, an *agrD* in-frame deletion was designed to generate a mutant unable to produce the putative autoinducer peptide processed from AgrD. As demonstrated in mutant DG125A (Δ*agrA*), no pleiotropic effect was observed in mutant DG119D (Δ*agrD*) (data not shown). Moreover, the adhesion phenotype of DG119D (Δ*agrD*) was similar to that of DG125A (Δ*agrA*) (Fig. 2A). Micrographs of the microscopic field of adhering cells on glass slides confirmed that the quantity of adhering cells with *L. monocytogenes* DG119D (Δ*agrD*) and DG125A (Δ*agrA*) was less compared to the parental strain EGD-e (Fig. 2B). These results suggested the involvement of the *agr* system during adhesion of *L. monocytogenes*, the first step in biofilm development.

The ability of *L. monocytogenes* EGD-e to develop biofilms on polystyrene was also affected by the deletion of *agrA* and *agrD* (Fig. 3). Indeed, there was significantly less biofilm ($n = 3$, $P < 0.05$) produced within the first 24 h of incubation. The differences were no longer significant during the later stages of biofilm formation, namely, at 48 and 72 h.

In light of the sessile growth alteration observed in the mutants with deletion in the genes encoding the putative transcriptional regulator AgrA and the putative autoinducer peptide processed from AgrD, we therefore decided to investigate the expression of the *agr* operon during sessile and planktonic growth.

Relative expression and transcriptional autoregulation of the genes of the *agr* operon. The transcription of the four genes of the *agr* operon was studied during sessile and planktonic growth using real-time PCR experiments with each of the four primer sets (Fig. 1A, b [BF2-BR2], d [DF2-DR2], c [CF2-CR2], and a [AF2-AR2], and Table 2). Analysis of the relative expression levels indicated that, during sessile growth, the levels of transcripts of *agrB*, *agrD*, and *agrC* were significantly lower ($n = 3$, $P < 0.05$) after 2 h of adhesion than after 24 and 72 h of sessile growth (Fig. 4A). For each gene, the differences

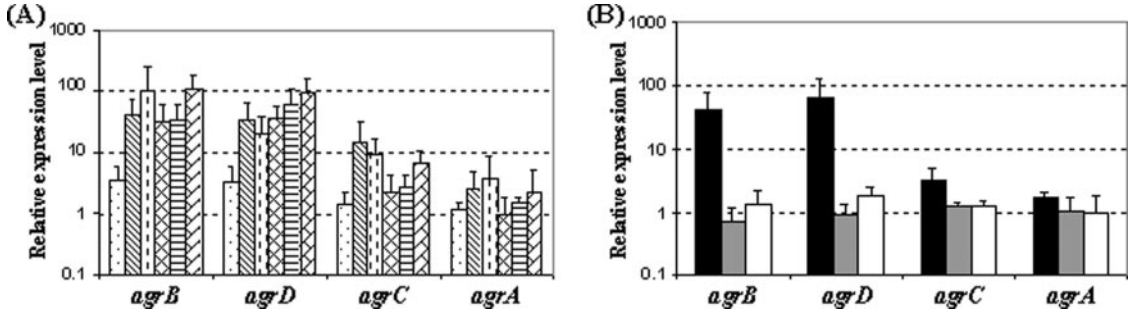

FIG. 4. Semilogarithmic representations. (A) Relative expression levels of the *agrB*, *agrD*, *agrC*, and *agrA* genes of the parental strain *L. monocytogenes* EGD-e determined during biofilm formation (2, 24, and 72 h [the first three columns in each gene, respectively] and planktonic growth (early exponential phase OD_{600} of 0.1, mid-exponential phase OD_{600} of 0.4, and stationary phase OD_{600} of 0.6 [the second three columns for each gene, respectively]). (B) Relative expression levels of the *agrB*, *agrD*, *agrC*, and *agrA* genes of *L. monocytogenes* determined during mid-exponential phase OD_{600} of 0.4: EGD-e strain (■), DG125A (Δ*agrA*) strain (▨), and DG119D (Δ*agrD*) strain (□). For both graphs, gene expression was quantified by using real-time PCR and the comparative critical threshold ($\Delta\Delta C_T$) method. The *drm* gene was used as the internal standard, and expression of the *agrA* gene in the early exponential phase (OD_{600} of 0.1) was used as the calibrator. Three independent experiments were performed; histograms indicate standard deviations.

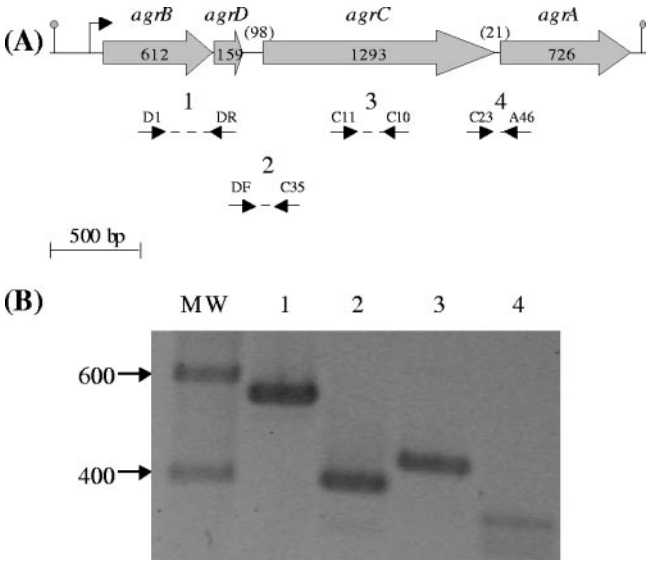

FIG. 5. RT-PCR analysis of RNA from *L. monocytogenes* cells at mid-exponential phase (OD_{600} of 0.4). (A) The dotted lines enclosed by arrows indicate the positions of the primers and PCR products. (B) The amplified products, lane numbers 1 to 4, were separated by electrophoresis on 1% agarose gel and correspond, respectively, to the expected sizes of 567, 388, 435, and 353 bp. The sizes of the DNA marker fragments are indicated in base pairs.

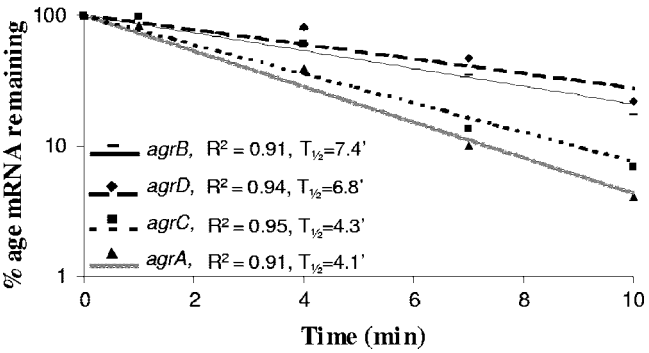

FIG. 6. Chemical half-life of the transcripts of the *agr* operon. Semilogarithmic plots of mRNA decay corresponding to the *agrB* (–), *agrD* (◆), *agrC* (■), and *agrA* (▲) genes. Total RNA was prepared 0, 1, 4, 7, and 10 min after treatment with rifampin (250 μg ml^{-1}). The results were obtained by real-time PCR analysis and normalized using 16S mRNA amounts. The correlation coefficient (R^2) and half-life ($t_{1/2}$) were determined for each regression analysis. Three independent experiments were carried out.

in the relative expression observed between 24 and 72 h of biofilm growth were not significant. The levels of *agrA* transcripts were similar at 2, 24, and 72 h. Furthermore, during sessile growth, for each condition, the levels of transcripts of *agrB*, *agrD*, and *agrC* were never significantly different. In contrast, the relative expression levels of *agrA*, for each condition, were significantly lower ($n = 3$, $P < 0.05$) than those of *agrB*, *agrD*, and *agrC*.

During planktonic growth, the relative expression levels of each gene was not affected by the phase of growth. The levels of transcripts of *agrB* and *agrD*, for each condition, were never significantly different. In contrast, the relative expression levels of *agrC* and *agrA*, for each condition, were significantly lower ($n = 3$, $P < 0.05$) than those of *agrB* and *agrD*. For example, under our experimental conditions, at mid-exponential growth phase (OD_{600} of 0.4) the *agrC* and *agrA* transcript levels were, respectively, 13- and 24-fold lower than the *agrB* transcript level (Fig. 4A).

The relative expression levels of the four genes of the *agr* operon were determined at mid-exponential phase during planktonic growth (OD_{600} of 0.4) in the parental and mutant (Δ*agrA* and Δ*agrD*) backgrounds. In mutant DG125A (Δ*agrA*), the relative expression levels of *agrB*, *agrD*, and *agrC* were significantly lower ($n = 3$, $P < 0.05$) than those of the parental strain EGD-e (Fig. 4B). Indeed, the relative transcript levels for *agrB*, *agrD*, and *agrC* were, respectively, of 56-, 68-, and 3-fold lower than those measured with the parental strain. A similar pattern of gene expression was observed for mutant DG119D (Δ*agrD*) (Fig. 4B). In terms of the relative expression levels of *agrA*, no significant differences were observed between the mutants (DG119D and DG125A) and parental strains. These results suggest an autoregulation of the transcription of *agrB*, *agrD*, and *agrC* and a low constitutive expression of the putative transcriptional regulator AgrA.

The mRNA quantification data suggested that the *agr* system was autoregulated and pointed to a differential expression of the *agr* genes during sessile and planktonic growth. Either posttranscriptional processing or transcription from another promoter region, not yet identified, could account for these results.

Processing of the mRNA and identification of the 5′ end of the mRNA *agr* operon. In order to further investigate the hypothesis of a posttranscriptional processing, RT-PCR, Northern blotting, and mRNA chemical half-life were carried out. The four genes and the two intergenic regions were detected by RT-PCR (Fig. 5), indicating cotranscription of the complete *agrBDCA* operon and the presence of a full-size transcript. PCR on the RNA samples before RT gave no amplification signals, confirming that there was no contamination by genomic DNA (data not shown). However, a polycistronic mRNA was never detected by Northern blotting; only small size products were detected (data not shown). The mRNA chemical half-life was determined by using real-time PCR experiments with the primer sets described above (Fig. 1A and Table 2). The results indicated that the chemical half-lives of *agrB* and *agrD* transcripts were 7.4 and 6.8 min, respectively, while they were lower for *agrC* and *agrA* (4.3 and 4.1 min, respectively) (Fig. 6). To pinpoint these differences in chemical half-life and to highlight the differential expression pattern observed by real-time PCR, 5′-RACE experiments were carried out to search for transcription initiation points or cleavages within *agrC* and *agrA* transcripts. Regardless of the treatment with TAP, multiple PCR products were detected, confirming degradation after cleavage through RNase activity. After amplification with adequate primers (Table 2), four 5′ ends were identified among the *agrC* fragments sequenced (Fig. 7). Similarly, five 5′ ends were observed among the *agrA* fragments sequenced (Fig. 7). From two hypotheses formulated, data analysis confirmed posttranscriptional cleavage and degradation.

5′-RACE was also used to characterize the 5′ end of the

FIG. 7. Analysis of the 5′ end of *agrB*, *agrC*, and *agrA* transcripts using total RNAs isolated from EGD-e cells collected during the exponential growth phase (OD_{600} of 0.4). #, 5′ end identified by primer extension; ∗, processing sites identified by 5′-RACE. The putative −10 with TGn extension and −35 sequences are double underlined, the ribosome binding sites are underlined, the start codons are boxed, and the stop codon of *agrC* is represented by three asterisks.

mRNA *agr* operon. PCR amplification was observed in TAP-treated and untreated samples, suggesting a processing event at the 5′ end, mapped by a "T" (Fig. 7). As expected, primer extension analysis with the three specific primers B34, B26, and B18 (Table 2) revealed two signals. They were separated by one nucleotide and corresponded to a "G" and the previously described "T." This finding suggested that the 5′ end of the *agr* transcript was located 15 or 14 nucleotides upstream from the putative start codon (Fig. 7). Similar results were obtained in samples harvested at an OD_{600} of 0.1, 0.4, and 0.6. Moreover, two hexanucleotides (TGGTTA and TAAAAT) separated by 18 nucleotides were detected upstream. They have similarities to the consensus −35 and −10 sequences of several promoters of housekeeping genes from gram-positive bacteria, as well as from *E. coli* (21, 23). Sequence conservation is higher in the −10 region than in the −35 region, and a TGn extension was observed upstream of the −10 region. Similar features were found in several promoters of gram-positive bacteria (20, 38).

DISCUSSION

Orthologs of the *agr* system, initially described in *S. aureus*, have been reported in *L. plantarum*, *E. faecalis*, and *L. monocytogenes* (6, 44, 48, 56). Thus far, the role of the *agr* system has not been clearly described in the pathogenic bacterium *L. monocytogenes*. In the present study, we investigated the role of *agrA* and *agrD* in the sessile growth of *L. monocytogenes*, and we focused on the molecular characterization of the transcription of the *agr* operon. In-frame deletions of *agrA*, which encodes a transcriptional regulator, or in-frame deletions of *agrD* encoding a propeptide affected adhesion and the early stages of biofilm formation on glass and polystyrene surfaces within the first 24 h of incubation. No significant differences were observed afterward. These results are in accordance with those obtained by Sturme et al. (48) with a *lamA* mutant of *L. plantarum* WCFS1. Indeed, the *lamA* mutant was impaired in its ability to adhere to glass surfaces. It showed 1.5- and 1.7-fold decreases in glass adherence compared to the parental strain after 24 and 48 h, respectively. In contrast, Vuong et al. (52), working with *S. aureus* RN6390 and 601055, demonstrated that their Δ*agr* genotype led to a pronounced attachment to polystyrene, 1.8- and 2.5-fold increases, respectively, compared to that of the isogenic *agr*$^+$ wild type after 24 h. Biofilm-associated infections have special clinical relevance, and in staphylococcal infections these diseases include endocarditis, osteomyelitis, implanted device-related infections, and even some skin infections (54). Indeed, the Δ*agr* biofilm phenotype may have important consequences. For example, the dysfunction of *agr* is correlated with persistent bacteremia in *S. aureus* (49), and mutation of the *S. aureus agr* system increased bacterial persistence (52), suggesting that interference with cell-cell communication would enhance rather than suppress this important type of staphylococcal disease (42).

In our experimental conditions, growth-phase-dependent transcriptional regulation was not observed during planktonic growth. This is in agreement with a previous report showed that during exponential and stationary phases the amount of *agrB* and *agrC* mRNAs was not significantly different (6), although a twofold difference in the quantity of *agrA* transcripts was recorded by these authors. In contrast, the transcription of the orthologous *agr*, *lam*, and *fsr* operons from *S. aureus* MN NJ, *L. plantarum* WCFS1, and *E. faecalis* OG1RF, respectively, increased from early to mid-exponential phase, suggesting growth-phase-dependent transcription upregulation (44, 48, 56).

During sessile growth, the transcription of the *agr* genes depended on the stage of biofilm development, suggesting that this system is important during biofilm development. Interestingly, a significant decrease in the transcript levels of *agrB*, *agrD*, and *agrC* was observed after initial attachment. At first glance, this may seem surprising since initial attachment is the step where *agr* impairment is most detrimental to biofilm formation; this points out that developmental regulations involved during sessile growth are complex (22). In *L. monocytogenes*, *agr*-dependent regulation may be transitory during biofilm formation as was observed in other systems. For example, two communication systems (*las* and *rhl*) play a role in transitional episodes in *Pseudomonas aeruginosa* biofilm development. The Las regulon is involved in early biofilm develop-

ment but not in later stages; in contrast, the Rhl regulon plays a role in the maturation of the biofilm (14, 46). The *agr* system of *L. monocytogenes* could also regulate the expression of proteins necessary for the ability to attach to abiotic surfaces without being involved once the cells attach to the surface. Indeed, in *S. aureus* and *S. epidermidis*, *agr*-dependent regulation of the expression of several adhesion proteins has been demonstrated (12, 34).

Significant differences were measured in the relative quantities of the transcripts of *agrB*, *agrD*, *agrC*, and *agrA*, while the differences between the transcripts of *agrB* and *agrD* were never significantly different. This observation suggested either posttranscriptional processing of the full-size *agr* transcript of *L. monocytogenes* or the presence of another promoter region between *agrD* and *agrC*. Determination of 5′ ends corresponding to cleavage, and not to initiation transcription points, supported the posttranscriptional events hypothesis. Indeed, several 5′ ends were detected within *agrC* and *agrA* transcripts. This suggested also that most of the transcripts quantified by real-time PCR were degradation products generated after cleavage of the full-length transcript, probably within the intergenic region or at the 5′ end of *agrC* and *agrA*. These posttranscriptional events may have regulatory functions resulting in a differential stability and a rapid processing of the mRNA. This could account for a fine tuning of the expression of the individual genes of the *agr* operon, as has previously been suggested for the pattern of expression of other loci of gram-negative and gram-positive bacteria (2, 24, 25, 37, 40). Moreover, our work indicated that the *agr* operon of *L. monocytogenes* was autoregulated in a positive way since the deletion of *agrA* or *agrD* reduced the transcription of *agrB*, *agrD*, and *agrC*, although *agrA* transcription was not *agr* dependent. A similar pattern has been described in the orthologous *fsr* system of *E. faecalis* in which the expression of *fsrB*, *fsrD*, and *fsrC* is *fsr* dependent, whereas the expression of the *fsrA* is weak, constitutive, and *fsr* independent (29, 45). It is proposed, on the one hand, that the regulator is constitutively expressed in order to provide a basal amount of regulator ready to respond to the presence of the signal in the environment of the cell; on the other hand, when the signal is high in the environment of the cell, it would induce the expression of the transmembrane protein, the propeptide and the sensor. This, in turn, would enable the transfer of the signal to the neighboring cells and prepare the cell for the monitoring of an amplified signal (18, 26).

Two 5′ ends of the *agr* mRNA were determined. One was mapped to a "G" and located at an appropriate distance downstream of the putative promoter region (43), leading us to consider it as the apparent start site for the promoter of the *agr* operon. The second 5′ end identified was located one base downstream of the 5′ end of the primary transcript. Such cleavage of one nucleotide downstream of the initiation site may derive from a modification of the primary transcript by a phosphatase or pyrophosphatase or from endonucleolytic cleavage (31, 47, 50, 51). The significance of such commonly observed processing remains to be clarified.

In conclusion, this study is the first description of the involvement of cell-cell communication in the adherence of *L. monocytogenes*. Our data show that impairment of the response regulator or the propeptide resulted in a similarly altered adhesion and biofilm phenotype. The *agr* system of *L. monocytogenes* differed from the homologous systems previously described since posttranscriptional processing occurred at the site of the initiation of transcription and within the full-length transcript. It will be of interest to investigate the significance of such a processing in the expression of the *agr* system and in the physiology of *L. monocytogenes*.

ACKNOWLEDGMENTS

This study was supported by the Ministère de l'Education Nationale de la Recherche et de la Technologie, the Université de Bourgogne, and the Institut National de la Recherche Agronomique.

We thank Sofia Kathariou for providing the pGF-EM vector, Philippe Gaudu for critical reading of the manuscript, and Mary Boulay for reading of the English text.

REFERENCES

1. **Aguado, V., A. I. Vitas, and I. Garcia-Jalon.** 2004. Characterization of *Listeria monocytogenes* and *Listeria innocua* from a vegetable processing plant by RAPD and REA. Int. J. Food Microbiol. **90:**341–347.
2. **Allenby, N. E. E., N. O'Connor, Z. Pragai, N. M. Carter, M. Miethke, S. Engelmann, M. Hecker, A. Wipat, A. C. Ward, and C. R. Harwood.** 2004. Post-transcriptional regulation of the *Bacillus subtilis pst* operon encoding a phosphate-specific ABC transporter. Microbiology **150:**2619–2628.
3. **Allison, D. G., B. Ruiz, C. San Jose, A. Jaspe, and P. Gilbert.** 1998. Extracellular products as mediators of the formation and detachment of *Pseudomonas fluorescens* biofilms. FEMS Microbiol. Lett. **167:**179–184.
4. **Arvidson, S., and K. Tegmark.** 2001. Regulation of virulence determinants in *Staphylococcus aureus*. Int. J. Med. Microbiol. **291:**159–170.
5. **Auger, S., E. Krin, S. Aymerich, and M. Gohar.** 2006. Autoinducer 2 affects biofilm formation by *Bacillus cereus*. Appl. Environ. Microbiol. **72:**937–941.
6. **Autret, N., C. Raynaud, I. Dubail, P. Berche, and A. Charbit.** 2003. Identification of the *agr* locus of *Listeria monocytogenes*: role in bacterial virulence. Infect. Immun. **71:**4463–4471.
7. **Balestrino, D., J. A. J. Haagensen, C. Rich, and C. Forestier.** 2005. Characterization of type 2 quorum sensing in *Klebsiella pneumoniae* and relationship with biofilm formation. J. Bacteriol. **187:**2870–2880.
8. **Bassler, B. L.** 2002. Small talk: cell-to-cell communication in bacteria. Cell **109:**421–424.
9. **Bensing, B. A., B. J. Meyer, and G. M. Dunny.** 1996. Sensitive detection of bacterial transcription initiation sites and differentiation from RNA processing sites in the pheromone-induced plasmid transfer system of *Enterococcus faecalis*. Proc. Natl. Acad. Sci. USA **93:**7794–7799.
10. **Bergmann, B., D. Raffelsbauer, M. Kuhn, M. Goetz, S. Hom, and W. Goebel.** 2002. InlA- but not InlB-mediated internalization of *Listeria monocytogenes* by non-phagocytic mammalian cells needs the support of other internalins. Mol. Microbiol. **43:**557–570.
11. **Challan Belval, S., L. Gal, S. Margiewes, D. Garmyn, P. Piveteau, and J. Guzzo.** 2006. Assessment of the roles of LuxS, *S*-ribosyl homocysteine, and autoinducer 2 in cell attachment during biofilm formation by *Listeria monocytogenes* EGD-e. Appl. Environ. Microbiol. **72:**2644–2650.
12. **Cramton, S. E., C. Gerke, N. F. Schnell, W. W. Nichols, and F. Gotz.** 1999. The intercellular adhesion (*ica*) locus is present in *Staphylococcus aureus* and is required for biofilm formation. Infect. Immun. **67:**5427–5433.
13. **Crossman, L., and J. M. Dow.** 2004. Biofilm formation and dispersal in *Xanthomonas campestris*. Microbes Infect. **6:**623–629.
14. **Davies, D. G., M. R. Parsek, J. P. Pearson, B. H. Iglewski, J. W. Costerton, and E. P. Greenberg.** 1998. The involvement of cell-to-cell signals in the development of bacterial biofilm. Science **280:**295–298.
15. **Desroche, N., C. Beltramo, and J. Guzzo.** 2005. Determination of an internal control to apply reverse transcription quantitative PCR to study stress response in the lactic acid bacterium *Oenococcus oeni*. J. Microbiol. Methods **60:**325–333.
16. **Djordjevic, D., M. Wiedmann, and L. A. McLandsborough.** 2002. Microtiter plate assay for assessment of *Listeria monocytogenes* biofilm formation. Appl. Environ. Microbiol. **68:**2950–2958.
17. **Donlan, R. M., and J. W. Costerton.** 2002. Biofilms: survival mechanisms of clinically relevant microorganisms. Clin. Microbiol. Rev. **15:**167–193.
18. **Dunn, A. K., and E. V. Stabb.** 2007. Beyond quorum sensing: the complexities of prokaryotic parliamentary procedures. Anal. Bioanal. Chem. **387:**391–398.
19. **Farber, J. M., and P. I. Peterkin.** 1991. *Listeria monocytogenes*, a food-borne pathogen. Microbiol. Rev. **55:**476–511.
20. **Garmyn, D., T. Ferain, N. Bernard, P. Hols, and J. Delcour.** 1995. Cloning, nucleotide sequence, and transcriptional analysis of the *Pediococcus acidilactici* L-(+)-lactate dehydrogenase gene. Appl. Environ. Microbiol. **61:**266–272.
21. **Guzzo, J., M.-P. Jobin, F. Delmas, L.-C. Fortier, D. Garmyn, R. Tourdot-**

Marechal, B. Lee, and C. Divies. 2000. Regulation of stress response in *Oenococcus oeni* as a function of environmental changes and growth phase. Int. J. Food Microbiol. **55:**27–31.
22. **Hall-Stoodley, L., and P. Stoodley.** 2002. Developmental regulation of microbial biofilms. Curr. Opin. Biotechnol. **13:**228–233.
23. **Harley, C. B., and R. P. Reynolds.** 1987. Analysis of *Escherichia coli* promoter sequences. Nucleic Acids Res. **15:**2343–2361.
24. **Hebermehl, M., and G. Klug.** 1998. Effect of oxygen on translation and posttranslational steps in expression of photosynthesis genes in *Rhodobacter capsulatus*. J. Bacteriol. **180:**3983–3987.
25. **Homuth, G., A. Mogk, and W. Schumann.** 1999. Post-transcriptional regulation of the *Bacillus subtilis dnaK* operon. Mol. Microbiol. **32:**1183–1197.
26. **Horswill, A. R., P. Stoodley, P. S. Stewart, and M. R. Parsek.** 2007. The effect of the chemical, biological, and physical environment on quorum sensing in structured microbial communities. Anal. Bioanal. Chem. **387:**371–380.
27. **Huber, B., K. Riedel, M. Hentzer, A. Heydorn, A. Gotschlich, M. Givskov, S. Molin, and L. Eberl.** 2001. The *cep* quorum-sensing system of *Burkholderia cepacia* H111 controls biofilm formation and swarming motility. Microbiology **147:**2517–2528.
28. **Jefferson, K. K.** 2004. What drives bacteria to produce a biofilm? FEMS Microbiol. Lett. **236:**163–173.
29. **Ji, G., R. C. Beavis, and R. P. Novick.** 1995. Cell density control of staphylococcal virulence mediated by an octapeptide pheromone. Proc. Natl. Acad. Sci. USA **92:**12055–12059.
30. **Kjelleberg, S., and S. Molin.** 2002. Is there a role for quorum sensing signals in bacterial biofilms? Curr. Opin. Microbiol. **5:**254–258.
31. **Kühn, K., A. Weihe, and T. Börner.** 2005. Multiple promoters are a common feature of mitochondrial genes in *Arabidopsis*. Nucleic Acids Res. **33:**337–346.
32. **Lawrence, L., and A. Gilmour.** 1995. Characterization of *Listeria monocytogenes* isolated from poultry products and from the poultry-processing environment by random amplification of polymorphic DNA and multilocus enzyme electrophoresis. Appl. Environ. Microbiol. **61:**2139–2144.
33. **Li, G., and S. Kathariou.** 2003. An improved cloning vector for construction of gene replacements in *Listeria monocytogenes*. Appl. Environ. Microbiol. **69:**3020–3023.
34. **Mack, D., A. P. Davies, L. G. Harris, H. Rohde, M. A. Horstkotte, and J. K. M. Knobloch.** 2007. Microbial interactions in *Staphylococcus epidermidis* biofilms. Anal. Bioanal. Chem. **387:**399–408.
35. **McNab, R., S. K. Ford, A. El-Sabaeny, B. Barbieri, G. S. Cook, and R. J. Lamont.** 2003. LuxS-based signaling in *Streptococcus gordonii*: autoinducer 2 controls carbohydrate metabolism and biofilm formation with *Porphyromonas gingivalis*. J. Bacteriol. **185:**274–284.
36. **Merritt, J., F. Qi, S. D. Goodman, M. H. Anderson, and W. Shi.** 2003. Mutation of *luxS* affects biofilm formation in *Streptococcus mutans*. Infect. Immun. **71:**1972–1979.
37. **Mongkolsuk, S., W. Panmanee, S. Atichartpongkul, P. Vattanaviboon, W. Whangsuk, M. Fuangthong, W. Eiamphungporn, R. Sukchawalit, and S. Utamapongchai.** 2002. The repressor for an organic peroxide-inducible operon is uniquely regulated at multiple levels. Mol. Microbiol. **44:**793–802.
38. **Murakami, S. K., S. Masuda, E. A. Campbell, O. Muzzin, and S. A. Darst.** 2002. Structural basis of transcription initiation: an RNA polymerase holoenzyme-DNA complex. Science **296:**1285–1290.
39. **Murray, E. G. D., R. A. Webb, and M. B. R. Swann.** 1926. A disease of rabbit characterised by a large mononuclear leucocytosis, caused by a hitherto undescribed bacillus: *Bacterium monocytogenes*. J. Pathol. Bacteriol. **29:**407–439.
40. **Nilsson, P., S. Naureckiene, and B. Uhlin.** 1996. Mutations affecting mRNA processing and fimbrial biogenesis in the *Escherichia coli pap* operon. J. Bacteriol. **178:**683–690.
41. **Novick, R. P., S. J. Projan, J. Kornblum, H. F. Ross, G. Ji, B. Kreiswirth, F. Vandenesch, and S. Moghazeh.** 1995. The *agr* P2 operon: an autocatalytic sensory transduction system in *Staphylococcus aureus*. Mol. Gen. Genet. **248:**446–458.
42. **Otto, M.** 2004. Quorum-sensing control in Staphylococci-a target for antimicrobial drug therapy? FEMS Microbiol. Lett. **241:**135–141.
43. **Phadtare, S., and K. Severinov.** 2005. Extended −10 motif is critical for activity of the *cspA* promoter but does not contribute to low-temperature transcription. J. Bacteriol. **187:**6584–6589.
44. **Qin, X., K. V. Singh, G. M. Weinstock, and B. E. Murray.** 2001. Characterization of *fsr*, a regulator controlling expression of gelatinase and serine protease in *Enterococcus faecalis* OG1RF. J. Bacteriol. **183:**3372–3382.
45. **Qin, X., K. V. Singh, G. M. Weinstock, and B. E. Murray.** 2000. Effects of *Enterococcus faecalis fsr* genes on production of gelatinase and a serine protease and virulence. Infect. Immun. **68:**2579–2586.
46. **Sauer, K., A. K. Camper, G. D. Ehrlich, J. W. Costerton, and D. G. Davies.** 2002. *Pseudomonas aeruginosa* displays multiple phenotypes during development as a biofilm. J. Bacteriol. **184:**1140–1154.
47. **Silvaggi, J. M., J. B. Perkins, and R. Losick.** 2005. Small untranslated RNA antitoxin in *Bacillus subtilis*. J. Bacteriol. **187:**6641–6650.
48. **Sturme, M. H. J., J. Nakayama, D. Molenaar, Y. Murakami, R. Kunugi, T. Fujii, E. E. Vaughan, M. Kleerebezem, and W. M. de Vos.** 2005. An *agr*-like two-component regulatory system in *Lactobacillus plantarum* is involved in production of a novel cyclic peptide and regulation of adherence. J. Bacteriol. **187:**5224–5235.
49. **Vance, G., J. Fowler, G. Sakoulas, L. M. McIntyre, V. G. Meka, R. D. Arbeit, C. H. Cabell, M. E. Stryjewski, G. M. Eliopoulos, L. B. Reller, G. R. Corey, T. Jones, N. Lucindo, M. R. Yeaman, and A. S. Bayer.** 2004. Persistent bacteremia due to methicillin-resistant *Staphylococcus aureus* infection is associated with *agr* dysfunction and low-level in vitro resistance to thrombin-induced platelet microbicidal protein. J. Infect. Dis. **190:**1140–1149.
50. **Vogel, J., I. M. Axmann, H. Herzel, and W. R. Hess.** 2003. Experimental and computational analysis of transcriptional start sites in the *Cyanobacterium prochlorococcus* MED4. Nucleic Acids Res. **31:**2890–2899.
51. **Vogel, J., V. Bartels, T. H. Tang, G. Churakov, J. G. Slagter-Jäger, A. Hüttenhofer, E. Gerhart, and H. Wagner.** 2003. RNomics in *Escherichia coli* detects new sRNA species and indicates parallel transcriptional output in bacteria. Nucleic Acids Res. **31:**6435–6443.
52. **Vuong, C., H. L. Saenz, F. Gotz, and M. Otto.** 2000. Impact of the *agr* quorum-sensing system on adherence to polystyrene in *Staphylococcus aureus*. J. Infect. Dis. **182:**1688–1693.
53. **Williams, T., S. Bauer, D. Beier, and M. Kuhn.** 2005. Construction and characterization of *Listeria monocytogenes* mutants with in-frame deletions in the response regulator genes identified in the genome sequence. Infect. Immun. **73:**3152–3159.
54. **Xu, L., H. Li, C. Vuong, V. Vadyvaloo, J. Wang, Y. Yao, M. Otto, and Q. Gao.** 2006. Role of the *luxS* quorum-sensing system in biofilm formation and virulence of *Staphylococcus epidermidis*. Infect. Immun. **74:**488–496.
55. **Yarwood, J. M., D. J. Bartels, E. M. Volper, and E. P. Greenberg.** 2004. Quorum sensing in *Staphylococcus aureus* biofilms. J. Bacteriol. **186:**1838–1850.
56. **Yarwood, J. M., J. K. McCormick, M. L. Paustian, V. Kapur, and P. M. Schlievert.** 2002. Repression of the *Staphylococcus aureus* accessory gene regulator in serum and in vivo. J. Bacteriol. **184:**1095–1101.
57. **Yarwood, J. M., and P. M. Schlievert.** 2003. Quorum sensing in *Staphylococcus* infections. J. Clin. Investig. **112:**1620–1625.